Rail and wheel health management

Citation for the original published paper (version of record):

Ekberg, A., Kabo, E., Lundén, R. (2023). Rail and wheel health management. Wear, 526-527.
http://dx.doi.org/10.1016/j.wear.2023.204891

N.B. When citing this work, cite the original published paper.

(article starts on next page)
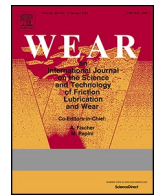
Rail and wheel health management

Anders Ekberg [*], Elena Kabo, Roger Lundén

CHARMEC, Chalmers University of Technology, SE-412 96, Gothenburg, Sweden

ABSTRACT

Rail and wheel health management is investigated with focus on deterioration phenomena in the wheel/rail contact interface – plastic deformation, wear, and rolling contact fatigue (RCF). How operational conditions affect deterioration, and how they can be included in wheel/rail health predictions is linked to a more in-depth description of deterioration mechanisms. Here means of measuring, quantifying, and predicting deterioration is in focus. This discussion provides the basis for the outline of a rail and wheel health management framework. As discussed in the paper, the proposed framework is well in line with the requirements in the ISO 55000 standard for asset management.

1. Introduction

A large proportion of railway maintenance costs relate to phenomena with origin in the wheel/rail interface, a fact that any asset management system must pay close attention to. Such a system should contain methods to monitor current status, predict how the status evolves over time, plan and carry out maintenance, and address any non-conformities. Establishing a rail oriented asset management system, even if it is limited to mechanical deterioration due to wheel/rail interaction, is therefore a vast and complex challenge. It requires a thorough understanding and suitable description of (existing and future) operational conditions, and all mechanisms of mechanical deterioration.

An efficient management strategy requires an interlinked use of monitoring data and numerical simulations. Here, key parameters and the precision/regularity with which they need to be measured/monitored need to be established. Monitoring and operational data should then be linked to numerical simulations to predict future status – an approach that in its evolved stage will form a digital twin.

The current study focuses on deterioration phenomena in the wheel/rail contact interface. It sets out by an overview discussion on how operational conditions can be characterised and quantified. This relates to the next sections on mechanical deterioration phenomena driven by the wheel/rail contact interaction, and how these phenomena can be monitored and numerically predicted. In this context, rail and wheel health management is discussed and contrasted to some key demands in international standards for asset management [1–3] and to risk analyses.

2. Operational conditions

An asset management system must set out from the prevailing operational conditions. In the case of wheel and rail health management, loading includes local wheel/rail contact forces, but also forces such as rail bending, which affect the entire rail cross-section. It also includes (global and local) thermal loads, and residual stresses from manufacturing and operation. Operational conditions further include geometry – both globally (track geometry) and on local (wheel and rail profiles) and very local (surface roughness) scales. In addition, there are environmental factors, such as wheel/rail friction, which have considerable effects on the deterioration.

A complete description of the operational conditions becomes unmanageable due to the large number of parameters that need to be accounted for. It is further aggravated by the fact that many influential parameters vary significantly over time and position, are correlated, and are difficult to measure. This calls for simplifications in excluding less influential parameters, optimisation of the time and spatial resolution, and estimation of influential parameters from measurable parameters. For mechanical deterioration related to wheel and rail interaction, establishing which simplifications that can be allowed is far from obvious. The reason is that many parameters are interdependent, and have an influence on several modes of deterioration. Further, the magnitude of influence varies with the degree of deterioration, cf. the discussion on the influence of lubrication in different stages of rolling contact fatigue (RCF) crack growth in Ref. [4]. As another example, one can consider plastic deformation of the wheel/rail contact surface, which will influence the contact geometry and thereby the dynamic

loads. This will cause an influence on subsequent deterioration in the form of additional plastic deformation, wear and RCF. This influence may be beneficial (e.g., improved distribution of contact stresses) and/or detrimental (e.g., deteriorated self-steering).

An overview of how some important operational conditions are related to different deterioration phenomena is presented in Fig. 1. It should be interpreted such that a 'global factor' (such as braking/traction) will have an effect on some 'local factors'. These will influence the deterioration phenomena that cause profile changes and cracks. In addition, high local thermal loads and plasticity may affect the material characteristics through transformation and hardening. A more detailed description is provided in chapter 3.

To define relevant operational conditions to include in track health predictions is another intricate challenge. On the one hand, the "worst" (often in a rather fuzzy statistical sense, e.g., with an estimated probability of occurring once in ten years) conditions are of interest especially with respect to maintaining safe operations and fulfilling legal demands. Traditionally, this is where the main focus has been. On the other hand, the "average" conditions (also often taken in a loose sense although stringent definitions may be found, see equation (1) below) are of interest when assessing the general decline in health and predicting larger maintenance actions. A suitable aim would be to include both of these aspects. Considering the development in sensor technology, data transmission, computational power, and the potential to carry out numerical simulations of deterioration, this has become more feasible. There are however considerations to be made in relation to the discussion on "worst" versus "average" conditions.

The scatter in operational loads is due to variations in vehicle and track characteristics. A "worst case loading" thus relates to a "worst case vehicle" in a "worst case track section", where "worst" will depend on the considered deterioration phenomenon. As an example, a dipped welded joint in combination with a heavy vehicle may be worst regarding fatigue, whereas a sharp curve and a stiff vehicle may be worst regarding wear. Further, condition most prone to accidents (i.e., derailments) may not be those causing the most severe deterioration. In the case of the curve above, a light vehicle with unbalanced loading would pose a large derailment risk, but may not induce the most wear.

To define an "average" condition is even more complex, and perhaps even irrelevant. The reason is that maintenance needs to be made before deterioration accelerates to unacceptable levels at some track sections or in some running gear. For this reason, it is more appropriate to divide track and vehicles into categories, for example the track can be categorised based on curve radii where different maintenance intervals are employed for different curve radii.
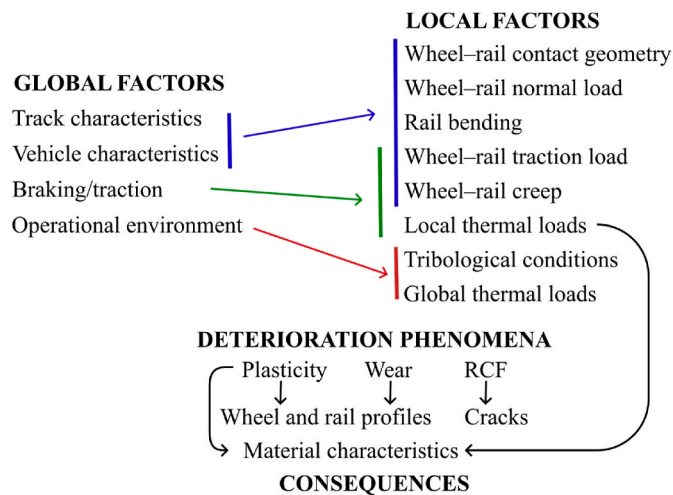
A second reason that the notion of an "average" vehicle – implicitly implied when maintenance is related to mega gross tonnes of traffic – is questionable since most, if not all, deterioration phenomena are exponential threshold phenomena. Here no (or very little) deterioration occurs as long as load levels are below the threshold. Above the threshold deterioration increases exponentially with the load. If all loads are above the threshold limit, a weighted average can be used to characterise the loads. As an example, the surface initiated RCF, life (see section 5.2) can be estimated as $FI_{surf} \approx 1.78(N)^{-1/4}$. A weighted average $\overline{FI_{surf}}$ for N load cycles of varying amplitude FI_{surf} can then be estimated (cf [5]. for the case of plain fatigue) as

$$\overline{FI_{surf}} = \left(\frac{\sum\limits_{i}^{N} \left(FI_{surf,i} \right)^4}{N} \right)^{1/4} \tag{1}$$

In conclusion, basing operational conditions on "worst" or "average" loads is challenging. The use of numerical simulations that allow the consideration of the entire load spectrum would seem to circumvent this. As discussed below, it will however require vastly more input data and, in particular, knowledge on which data that are required and how to employ the data. The analyses also need to consider correlations between different load (and other operational) parameters especially if risks of failures should be assessed. The topic is further discussed in relation to the influence of track upgrading in Refs. [6,7].

Finally note that also operational conditions other than mechanical loads (e.g., temperature) have to be related to their influence on the operational load magnitudes and/or material resistance. Once that (sometimes very complex) translation is done, the considerations above are valid.

3. Managing mechanical deterioration

Wheels and rails need to fulfil performance demands, which will depend on operational conditions. As deterioration progresses, the wheels and rails will be less able to fulfil these demands. A common way to address this in an asset management system is through periodic maintenance together with alert and safety limits. This can be a rather crude approach due to the often strict division into acceptable and unacceptable levels, and the need to base maintenance intervals on the most detrimental operational conditions. A more refined approach is the use of predictive maintenance where the evolution of degradation is predicted beforehand to allow for improved maintenance planning. Ideally, the health status of wheels and rails should then never (or at least very seldom) deteriorate to exceed alert and safety limits.

To enable predictive maintenance (and also to adhere to alert and safety limits), it is vital to monitor the current health status related to relevant deterioration phenomena. In the following we will discuss some of these damage phenomena. Possibilities to characterise, inspect, and predict the related deterioration are especially considered. We will then come back to the relation to asset management, and investigate links to current standards in chapter 8.

4. Mechanical deterioration due to plastic deformation and wear

Plastic deformation and wear will modify rail head and wheel tread geometry. The modification may affect the transverse profile and/or the longitudinal/circumferential profile. This influences vehicle steering ability, contact forces and contact stresses, which all influence the magnitude of additional deterioration in the form of plastic deformation, RCF and wear. The influence may be beneficial (e.g., wear-off of initiated cracks, or profile adaptation that increases the contact patch size) or detrimental (e.g., periodic wear that increases dynamic loads). Plastic deformation and wear can be more or less evenly distributed over longer

Fig. 1. Relations between global operational conditions, local influencing factors, subsequent phenomena, and resulting consequences.

distances (e.g., flange or gauge corner wear), or be localised (e.g., dents) or periodic (e.g., corrugation, out-of-roundness). Distributed profile changes will influence contact geometry which may affect steering, contact stress magnitudes etc. whereas local and periodic geometry changes typically increase dynamic wheel/rail contact loads.

4.1. Status characterisation of plastic deformation and wear

Profile measurements can be employed to quantify the deterioration. Here material loss in the entire rail head/wheel tread needs to be quantified if plastic deformation (that causes profile modification without volume loss) should be distinguished from wear. The distinction between material loss due to wear or cracking is not perfectly well defined, but in general wear corresponds to a much more gradual (and more shallow) loss of material. A detailed visual inspection will distinguish "smoother" worn surfaces from the more "ragged" surfaces caused by RCF material fall-out.

Rail and wheel profile deterioration is commonly quantified (and restricted) by safety related measures, such as rail gauge and flange width. From a maintenance perspective, it is however more suitable to base the characterisation on the influence on subsequent wear and cracking of rails and wheels, see Refs. [8,9]. A challenge in profile measurements is to relate the worn profile to the nominal profile. For wheels (not on trams) the flange tip/field side are commonly used as height/width references. On rails, the field side can be used in a similar manner, but the height level is more undetermined as rail head wear will occur.

For (more or less) periodic wear and/or plastic deformations, amplitude and wavelength of rail irregularities are of importance, see e. g., Refs. [10–12]. On rail, these quantities can be measured using trolleys [13], or (especially for longer irregularities) by vehicle based measurements, see e.g., Ref. [14]. For wheels, profiles are commonly measured using mechanical probes, although laser scanning is gaining in precision and popularity, see e.g., Ref. [15]. Also axle box accelerations can be employed as an indirect measure of the effect the geometry has on (mainly vertical) track forces.

In addition to profile changes, plastic deformations will induce residual stresses and cause material hardening/softening. One straightforward way to estimate these effects is through hardness measurements. For more detailed analyses there are a multitude of (destructive and non-destructive) methods to measure residual stresses, see e.g., Ref. [16].
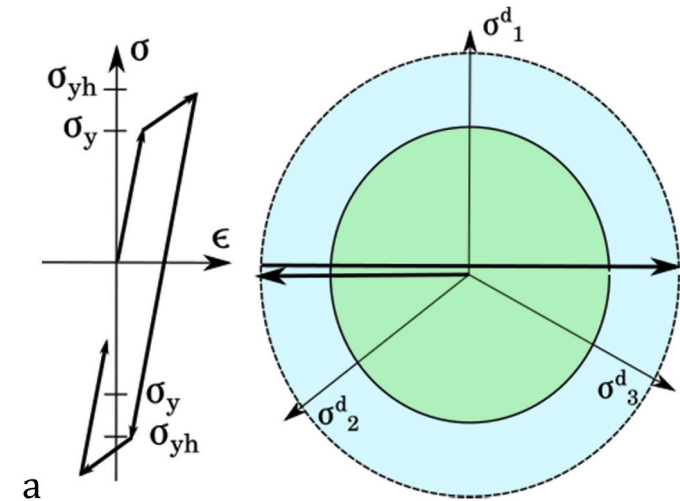
4.2. Prediction of plastic deformation and wear

Plastic (irreversible) deformation will occur once the stress exceeds a certain magnitude – the yield limit, σ_y. In railway applications, and particular regarding the wheel/rail contact, the situation is complicated by the fact that the loading is multiaxial, cyclic and compressive. Under multiaxial conditions, the state of stress and strain needs to be quantified by effective stress and strain measures, commonly the von Mises stress which states that plasticity occurs if $\sigma_{vM} = \sqrt{\frac{3}{2}\sigma_{ij}^d \sigma_{ij}^d} > \sigma_y$, where σ_{ij}^d is the deviatoric stress tensor. The resulting plastic deformations can be evaluated from finite element simulations.

Under repeated cyclic loading the material will soften or harden, meaning that σ_y will evolve over time, often in a fairly complex manner that is also affected by larger temperature variations, see Ref. [17]. For modelling purposes, hardening (and softening) are commonly divided into isotropic (that imposes overall hardening) and kinematic (that shifts the yield surface) parts, see Fig. 2. In wheel/rail contacts kinematic tends to dominate and saturation of hardening tends to occur.

Material hardening and residual stresses will limit subsequent
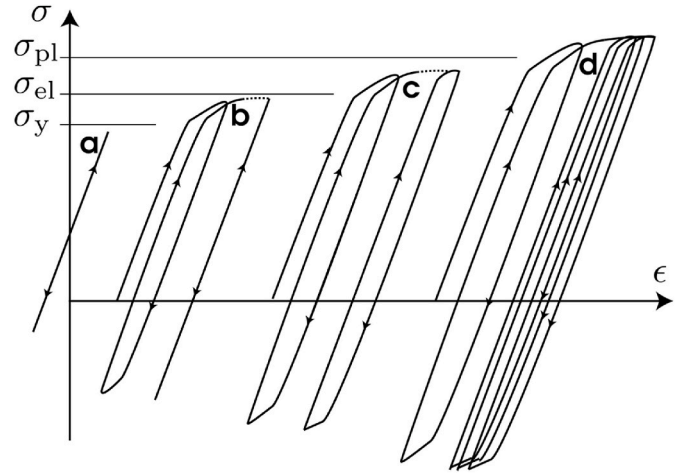
Fig. 3. Conceptual material response due to constant amplitude cyclic stresses exceeding the initial yield limit σ_y. a) elastic, b) elastic shakedown (up to the limit σ_{el}), c) plastic shakedown (up to the limit σ_{pl}), d) ratcheting.

Fig. 2. Conceptual stress evolution in the case of a) isotropic and b) kinematic hardening. Here σ and ε are stress and strain, σ_y initial and σ_{yh} evolved yield stress under cyclic loading. Further, σ_1^d, σ_2^d and σ_3^d are the deviatoric principal stresses. In the figures to the right, the yield limit initially (green), after half a load cycle (blue) and after a full load cycle (yellow) are indicated. The solid horizontal arrows indicate the applied load. (For interpretation of the references to colour in this figure legend, the reader is referred to the Web version of this article.)

plasticity, see Fig. 3. If sufficient, a state of elastic (no plastic deformations) or plastic (no plastic strain accumulation) shakedown will occur. If not confined, plastic strain accumulation (ratcheting) on wheel and rail surfaces will eventually cause surface initiated rolling contact fatigue cracking, see Ref. [18] for detailed discussions.

The compressive loading in the wheel/rail contact allows the plastic deformation to be very high before (ratcheting) failure occurs. In combination with non-symmetric (directional) loading e.g., due to braking/traction this makes anisotropic hardening important. Anisotropic hardening makes the yield limit orientation dependent – in Fig. 2 this would correspond to elliptic yield surfaces. To capture this phenomenon in numerical simulations requires sophisticated constitutive models, see Ref. [19]. Material anisotropy is also likely to affect the resistance to crack initiation and growth, cf [20].

For wear predictions, the Archard model [21] evaluates wear volume as

$$V_{\mathrm{w}} = k \frac{P\delta}{H} \tag{2}$$

Here V_{w} is the volume of wear, P the normal force, δ the wheel/rail sliding distance, H the hardness of the softer material and k a wear coefficient that will depend on contacting materials, sliding speed, contact pressure etc.

The $T\gamma$ model [22] evaluates wear and RCF damage from the tangential wheel/rail contact conditions

$$D = f(T\gamma) \tag{3}$$

Here T is the creep force, γ creep, and D damage evaluated from a trilinear damage function f. In wheel/rail contact cases where spin plays an important role, equation (3) can be employed locally to account for spin, see e.g., Ref. [23].

It is seen that both models employ wheel/rail sliding or creep. Further, they include the tangential or normal load where the latter implicitly relates to the frictional force through the inclusion of sliding. Important factors such as contact geometry, temperature, surface conditions etc. are implicitly included in the wear coefficient k in the Archard model, and in the trilinear damage function, f in the $T\gamma$ model. Consequently, the models need to be calibrated for different operational conditions. For k, this is commonly evaluated in lab tests and reported in so-called wear maps [24], whereas the $T\gamma$ model needs to be calibrated from field data [25].

It can be noted that also local wear (e.g., at welds) can be predicted using the Archard wear model if k is calibrated for the local conditions. The $T\gamma$ model is less suited for such predictions since the damage function is more complex to calibrate towards local conditions as it accounts for both wear and RCF damage, see section 5.2.

5. Material deterioration due to fatigue cracking

The highly dynamic loading of wheel and rail may cause fatigue crack initiation and growth. In parts of the rail section that are relatively far from the wheel/rail contact, *plain fatigue* may occur – this type of deterioration is considered out-of-scope for the current paper.

Closer to the wheel/rail contact patch, the rolling/sliding contact between wheel and rail may cause RCF cracks. For a broad overview of the phenomenon, its causes and consequences, see e.g., Ref. [26]. *Surface initiated RCF* is mainly a low cycle (i.e. plastic strain driven) fatigue phenomenon where crack initiation is usually related to ratcheting, see Figs. 3 and 4a. Cracks grow into the rail head at a fairly shallow angle and may at a depth of some millimetres deviate towards the surface (causing pitting) or transversally (causing a rail break). Surface irregularities will aggravate the situation, especially for cracks of squat type [27], see Fig. 4b. In addition, cold ambient temperatures may have significant effects on crack initiation [28], as well as on crack growth and final fracture in rails [29]. Initiation of *subsurface initiated RCF* cracks is mainly a high cycle fatigue phenomenon. The subsurface stress magnitude is highly influenced by the surface geometry and the normal (vertical) load. The fatigue resistance is locally decreased by occurring material defects.

Thermal cracks occur at the wheel or rail surface when the temperature is locally very high typically due to excessive wheel/rail sliding. The restricted expansion of the (small) heated volume produces compressive stresses that may be high enough to cause plastic yielding. During cooling, this will lead to the formation of tensile residual stresses that may cause (quasi-static) propagation of small surface defects [30]. Due to the directions of the (dominating) residual stress along the rail or around the wheel, the thermal cracks tend to extend transversally into the rail/wheel material. At high temperatures, martensite may form, and will promote subsequent crack initiation, see Ref. [27].

Unless the entire wheel is overheated, thermal cracks typically occur in localised spots, see Ref. [28] and Fig. 5. Subsequent propagation of thermal cracks is due to repeated rolling contact stresses unless additional thermal overloads occur. This implies that if the loading conditions are sufficiently benign in respect to surface initiated RCF, thermally induced cracks may wear off. In Fig. 5 this is however not the case. The wheel life may then be substantially reduced since thermal cracks may occur also at new, undamaged wheels and rails.

5.1. Status characterisation of fatigue cracking

Status characterisation of rail cracks should prevent large material detachment and fracture of wheels and rails, and aid in planning maintenance in the form of reprofiling. Inspections are however costly and may interfer with operational traffic. To balance these issues and

Fig. 4. a) Headchecks on the rail gauge corner. b) Squats on the railhead (right).

Fig. 5. Thermal facets (dark regions) on top of bands of surface initiated RCF.

develop an 'optimised' inspection strategy, risk and economical analyses can be employed, see e.g., Ref. [31]. Such an analysis requires a number of parameters that have to be estimated. One key factor is the accuracy of the crack inspection method. There are today a number of such methods available, each with pros and cons, as discussed below. Additional information can be found e.g., in the overview of non-destructive test methods presented by the European project INNOTRACK [32]. Note that the summary below only discusses the ability to detect/characterise cracks. In addition, all methods face the difficulty of establishing the position of detected cracks. Further, the detection results can be presented in different ways. Here aggregated results ('crack densities') may be suited for maintenance purposes, whereas identification of the deepest cracks is more suitable from a safety perspective.

Ultrasonic testing is a common technology to detect relatively large defects in rails and wheels, typically with a focus on managing RCF cracks [33], or performing quality controls at manufacturing or reprofiling. Ultrasonic testing employs a beam of ultrasonic energy transmitted into the rail. Defects are detected from reflection/scatter of this energy. To enhance the accuracy, energy is transmitted at different incidence angles. Operational inspections by trains at speeds up to some 70 km/h and in tests up to 100 km/h are reported in Ref. [32]. Ultrasonic testing is sensitive to distortions in the transmission interface. Similar to eddy current measurements (see below), variations in the stand-off distance between the transducer and the rail will influence the measurement results, see e.g., Ref. [34]. The method is useful for detecting deep cracks, but less successful for more shallow cracks. Also, surface cracks may block deeper crack, thereby limiting detectability of these [35]. In Refs. [34,36] it is discussed how this effect can be reduced by the use of multifrequency Rayleigh waves where higher frequency waves are trapped by the shallow cracks, whereas lower frequency waves extend to the deeper cracks.

One way of generating and detecting ultrasound while removing the need for a couplant between transducer and rail (which limits inspection speeds) is the use of electromagnetic acoustic transducers that employ a strong magnetic field and pass a large current pulse through an inductive coil in close proximity to a conducting surface [32,36]. In Ref. [32] inspection speeds of 10–15 km/h are discussed. In Refs. [34,36] 'pitch–catch' schemes of two separated (arrays of) electromagnetic acoustic transducers are presented. This allows inspections at higher speeds since the pitched ultrasonic wave is picked up by a separate transducer and therefor will not require the (single) transducer to stay in position for the transmitted pulse to be detected. Another way of remotely generating ultrasonic waves is through the use of a pulsed laser. Tests up to some 30 km/h (but with optimum speeds up to 15 km/h) with pulsed lasers are reported in Ref. [32].

Ultrasonic inspections can be enhanced by combining multiple ultrasonic elements and time delays in an ultrasonic phased array. This allows to steer, scan and focus the ultrasonic beam [32]. The ultrasonic waves can also be transmitted along the rail to provide long-range inspections through the use of guided wave technology. The long-range ability (up to 180 m according to Ref. [32]) is highly affected by several factors and will require a crack that significantly reduces the cross-sectional area (5% stated in Ref. [32], whereas 15% of the head area is stated in Ref. [37]) to provide an interpretable indication. Such long-range inspections could also (at least in theory) be employed to identify rail foot cracks, see the numerical investigation in Ref. [38].

Eddy current testing relies on the principle that the impedance of a coil containing an alternating current will be altered if the magnetic flux through the coil is influenced by the proximity of an electrically conductive material. The impedance change will be affected by a number of parameters including size, location, shape and properties of flaws in the electrically conductive material, see Ref. [39]. An eddy current probe containing two pickup coils wound in opposite directions should in theory balance essentially all influencing factors except those of sharp defects [39,40], but in reality, interaction between defects etc. makes this less efficient. Eddy current density decays exponentially below the surface, which makes the method mainly suitable for identifying fairly shallow surface cracks [41]. A penetration depth of 3 mm has been indicated as a practical limit [42] with a note that the resolution decreases exponentially with depth. This resolution is highly influenced by inspection conditions – under laboratory conditions, detection of cracks down to (at least) 5 mm are reported in the literature [43]. The eddy current probes can be calibrated to evaluate the length of the crack, but will then require knowledge of the growth angle (which ranges between roughly 15°–30°) to be able to asses crack depth (and vice versa). Eddy current inspections can be performed at rather high speeds. Inspections at 70 km/h are mentioned in Ref. [41].

Magnetic flux leakage features a magnetic sensor array that detects when the applied magnetic field interacts with surface (or shallow subsurface) discontinuities. Magnetic flux leakage was found to be able to identify surface features of artificial multiple surface cracks to some degree [44], but was less accurate with natural cracks. In these tests it was not able to identify crack depths. In Ref. [32] it is reported that magnetic flux leakage methods are used in combination with ultrasonics for inspections at around 35 km/h.

Thermography methods employ that loading of a rail will induce a small temperature increase in the compressed region, and a similar decrease in temperature in the region subjected to tensile stresses [45]. At a rail crack, the temperature change is magnified due to the stress concentration. This temperature peak can be employed to identify surface cracks, as shown e.g., in Ref. [45]. By using pulsed eddy currents to heat the material, thermography can be added as an additional means of crack detection [46,47]. Naturally, this will require some heating period of the material. In Ref. [48] it was shown that the thermal contrast decreased roughly proportionally with the square root of the speed of the passing heat source. The theoretical assessment was confirmed by experiments performed at train speeds 2–15 km/h.

When an *alternating current field* is induced in a thin layer near the surface, a surface defect will disturb the current flow and can thereby be detected. According to Ref. [32] alternating current measurements are less sensitive to maintaining a close and constant distance between sensors and the inspected component. Rail inspection speeds of some 2–3 km/h are reported in Ref. [32]. A special case here is the electromagnetic tomography investigated in Ref. [49]. The principle is that an alternating current field is employed to extract detailed defect information. However, since the sensor coils cannot encircle the rail, the sensor structure has to be modified to an L-shaped array covering the gauge corner. In Ref. [49] the methodology is tested in a laboratory set-up.

Visual crack inspections carried out by experienced staff have been, and are still, very common. To decrease time in track and provide more 'uniform' evaluations, there have for some time been investigations in

enhancing (automated) visual inspections by image analysis. In theory, the speed of inspection is then limited by the ability of the video camera to obtain images with sufficient resolution. One of the major challenges of visual/image based analyses is to distinguish between initiated cracks (e.g., RCF cracks) and benign but similar surface features (e.g., grinding marks or dirt) [50]. Various forms of image processing can be employed to increase the ability to distinguish between these, see e.g. Ref. [51], but in general the challenges are significant in uncontrolled environments. The situation can be significantly improved if digital image correlation is employed to evaluate the strain concentrations emanating from surface-breaking cracks, see Ref. [52]. This approach will also allow for estimating the crack depth.

Investigations in Ref. [53] showed how high energy *X-ray 3D reconstruction* provided an accurate main crack geometry, but had problems identifying tightly closed parts of the crack, in particular close to the crack tip. The extension to *X-ray tomography* provided topographic information, but required the extraction of a smaller sample cut out from the rail head.

Abilities of the different rail crack detection techniques are summarized in Table 1, which shortens and updates the summary in Ref. [32]. Note that the features are representative for 'standard' systems – many drawbacks and limitations can be overcome by modification of equipment, measurement principles or by post-processing of results from several measurements, as discussed above. Note also that accuracy typically decreases with increased speed, and that the 'accuracy' will depend on which features that are investigated. Finally note that there are also possibilities to use e.g., axle box accelerations as an indirect measure of the effect the cracked geometry has on (mainly vertical) track forces.

5.2. Prediction of fatigue cracking

Prediction of *surface initiated RCF* is generally based on either the $T\gamma$-approach (in essence an analysis based on the amount of energy submitted to the contact patch), shakedown analysis (in essence an analysis of whether there will be plastic deformation in the contact surfaces), or multiaxial low cycle fatigue/ratcheting analysis.

The $T\gamma$-approach evaluates the product of the creep force and the creep (sometimes extended to account for spin [23]). The resulting energy measure is related to wear and RCF life through a trilinear damage function, see Ref. [22] and equation (3).

The shakedown approach compares the applied friction (through the traction coefficient, f) towards the contact pressure normalised by the yield limit in cyclic shear. Frictional stress magnitudes inducing plastic deformation at the surface (to the right of the thick line in Fig. 6) are identified as prone to induce surface initiated RCF [18]. This criterion can (with some assumptions) be translated to a fatigue index [54]

$$FI_{\text{surf}} = f - \frac{2\pi abk}{3P} \tag{4}$$

Table 1
Rough summary of main features of some different non-destructive rail defect inspection technologies.

| Technique	Speed	Detection depth	Accuracy
Ultrasonics	fast ($\sim$ 70 km/h)	deep, but not very shallow	high
Eddy current	fast ($\sim$ 70 km/h)	several millimetres	high
Magnetic flux leakage	medium ($\sim$ 35 km/h)	surface features	medium
Thermo-graphy	low	surface features	medium
Alternating current field	low	some millimetres	medium
Visual (video) inspections	very fast (>300 km/h)	surface features	low
X-ray	very low	depends on power/time	very high
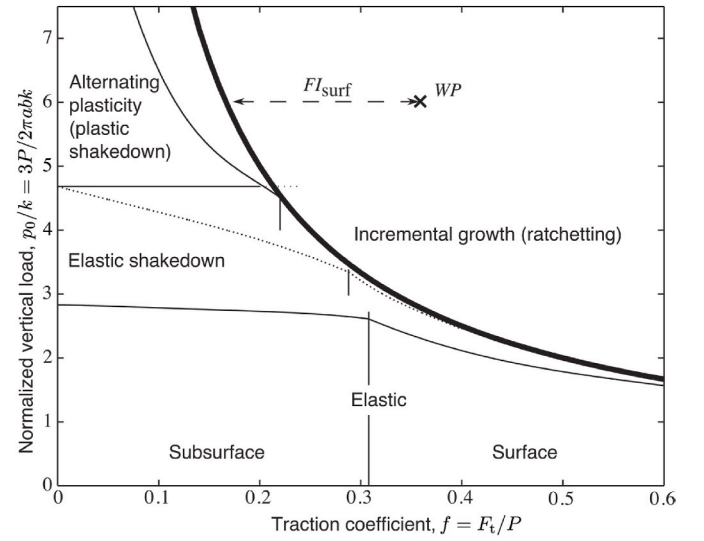
Fig. 6. Shakedown diagram [18,56]. Load conditions (WP – working point) outside thick line induce surface plasticity (and eventually surface initiated RCF). FI_{surf} according to equation (4) is indicated by a dashed line.

where f is the traction coefficient, a and b are semi-axes of the contact patch, k the yield limit in cyclic shear and P the normal force. The resulting fatigue life, N, (or corresponding fatigue damage) can be estimated using an equivalent Wöhler curve [55]

$$FI_{\text{surf}} \approx 1.78(N)^{-0.25} \leftrightarrow D \approx \frac{\left(FI_{\text{surf}}\right)^4}{10} \tag{5}$$

Here $D \equiv 1/N$ is the fatigue damage. For varying FI_{surf} magnitudes, damage is usually presumed to accumulate linearly for passing wheels (rail) or wheel revolutions (wheel), see Ref. [4] for a more detailed discussion.

In more explicit analyses of the material deformation during rolling contact, multiaxial low cycle fatigue can be analysed using e.g., the Jiang–Sehitoglu criterion, see [57].

$$FP = \left\langle \frac{\Delta\varepsilon}{2}\sigma_{max} \right\rangle + c_j \Delta\gamma \Delta\tau \tag{6}$$

where for a given shear plane, $\Delta\varepsilon$ is the normal strain range, $\sigma_{\max}$ is the maximum (over time) normal stress, c_j is material parameter, $\Delta\gamma$ is the shear strain range and $\Delta\tau$ the shear stress range. FP is a fatigue parameter that can be related to the fatigue life, N, as

$$(FP - FP_0)^m N = C \tag{7}$$

where FP_0, m and C are material parameters. An application example is provided in Ref. [55].

More commonly, surface initiated RCF occurs as a consequence of ratcheting, which can be predicted from numerically evaluated stress–strain responses during rolling contact using the Kapoor criterion [58].

$$\sum_i \Delta\varepsilon_{ri} = \varepsilon_c \tag{8}$$

Here $\Delta\varepsilon_{ri}$ is the plastic strain increment at load cycle i, and ε_c is the fracture strain. An example of applying this criterion for RCF predictions is presented in Ref. [30] where it is found that low cycle fatigue and (especially) ratcheting predictions are highly sensitive to the employed constitutive model of the rail/wheel material.

Methods to predict crack growth directions under the complex conditions prevailing in the wheel/rail contact zone are presented in Ref. [59]. Predictions become simpler and more reliable for railhead

cracks deviated to transverse growth. Such cracks essentially grow in plain fatigue where growth rates can be predicted using (variations of) Paris law, see Ref. [29].

Initiation of *subsurface initiated RCF* is generally predicted using a multiaxial high cycle fatigue criterion. In Ref. [60] the Dang Van criterion was employed and extended to predict fatigue damage. The fairly involved derivation of the Dang Van equivalent stress, σ_{dv}, was in Ref. [54] simplified to a fatigue index

$$FI_{sub} = \sigma_{dv} \approx \frac{P}{4\pi ab} \tag{9}$$

Here P is the contact load, and a and b semi-axes of the Hertzian contact patch. Fatigue is predicted for $\sigma_{dv} > \sigma_{edv}$ where σ_{edv} is the equivalent fatigue limit reduced to account for the occurrence of material defects, see Ref. [4].

After an initial period of tensile driven growth, see Ref. [61], subsurface initiated RCF crack growth is shear driven, after which it may deviate to transverse growth. Predictions of crack growth are thus similarly complex as for short surface initiated RCF cracks with the added complexity that the crack face friction is not reduced by liquid penetration.

Initiation of *thermal cracks* typically occurs as quasi-static fracture. Tensile residual stress formation as a consequence of the heating may be predicted using thermomechanical finite element simulations that may need to include phase transformations, see e.g., Ref. [62]. To predict if crack propagation of surface defects will occur, and to which depth, a fracture mechanics approach may be employed [63]. For rails the heating events are usually more short-term than in wheels, which results in a more shallow thermally affected zone and thus shallower thermal cracks.

6. Deterioration not related to plain rails and wheels

Rail joints impose discontinuities in the (running surface of the) rail, which cause increased dynamic loads and contact pressures. In addition, insulated joints feature fishplates that alter mass and stiffness of the rail section, which increases the dynamic loading further. The high dynamic load may also cause settlements with additional increases in loads and deterioration as consequences.

The locally high stresses can cause early plastic deformation and crack initiation at the rail ends of the running surface, see Ref. [64]. The very low load carrying capacity of the insulating layer will not limit the plastic flow [65]. The consequence may be lipping at the rail ends that may bridge the joint and cause short-circuiting. Status characterisation and prediction can be made using methods outlined above if dynamic loads due to the (dipped) joint, and the influence of the free rail surfaces are accounted for.

Switches & crossings are here similar in that they impose discontinuities in the rail, and consist of components with load application close to free surfaces. Also for switches & crossings, the methods described above can be employed to assess and predict deterioration if the (deteriorated) geometries are accounted for. There are additional deterioration mechanisms related to driving and locking devices, but these are deemed to be outside the scope of the current paper.

Correctly manufactured *welds* should not impose any distortion in the rail geometry. However, the introduction of a weld material and a heat affected zone may cause differential wear (cupping). Further, welding induces high tensile residual stresses, and material impurities. This increases the risk of subsurface RCF, and plain fatigue in the rail web and foot. Also here, methods for characterisation and prediction of subsequent deterioration discussed above can be employed if the influences of altered wear resistance, material defects, residual stresses, and cupping are accounted for, see e.g., Refs. [66,67].

7. Rail and wheel health management strategies

Rail and wheel health management includes quantification of current, and prediction of future health status. It should be supported with a monitoring/inspection strategy that specifies what should be monitored, and with which precision. Fig. 1 provides an overview of influential factors. Most of the local factors are not directly measurable, or can only be evaluated point-wise. This means that any rail and wheel health management strategy has to include some simulations in the sense that observable data must be transferred to influencing parameters and subsequent quantifications of rail and wheel deterioration.

The ability to identify, monitor and predict the evolution of key health parameters allows for the creation of digital twins. This concept has often been (mis)used to also include databases and stand-alone models, as visualised in the proposed classification of Fig. 7. The focus of the current study is on levels 5 and 6 where updated simulation models are employed to predict maintenance/inspection needs (5), and measured deterioration is employed to enhance the predictive ability (6). In contrast, level 4 implies a simulation model calibrated for current operational conditions, and level 7 a digital twin that makes unsupervised maintenance decisions.

As a concrete example, consider initiation of surface initiated RCF. Referring to equations (4) and (5), lateral and normal forces, and the contact patch size will characterise the load. To obtain these, multibody dynamics simulations are typically performed. However, vehicle and track characteristics will evolve over time, which will affect operational loads and profiles of wheels and rails. In this process, a rail section will be affected by all passing wheels, whereas a certain wheel will be subjected to the influence of all traversed track sections, which causes the complexity in detailed analyses to become very large especially in mixed traffic. There will thus be a need for simplifications. The most extreme approach is to presume steady-state conditions and ignore all but one (or a few) operational parameters. This is the philosophy behind maintenance scheduling based on e.g., total load (MGT) and/or curve radius.

To improve such rough measures, physical modelling can be used to characterise how safety and deterioration levels are affected by a key parameter. This is the implicit philosophy behind alarm, and maintenance limits. A more advanced approach is using simulations to characterise the combined influence of key characteristics. An example for surface initiated RCF is the use of meta-models based on parameterised wheel and rail profiles, see Refs. [8,9]. Taking this even further, is the possibility of simulating evolving wear, RCF etc. during operations using combinations of simulation models.
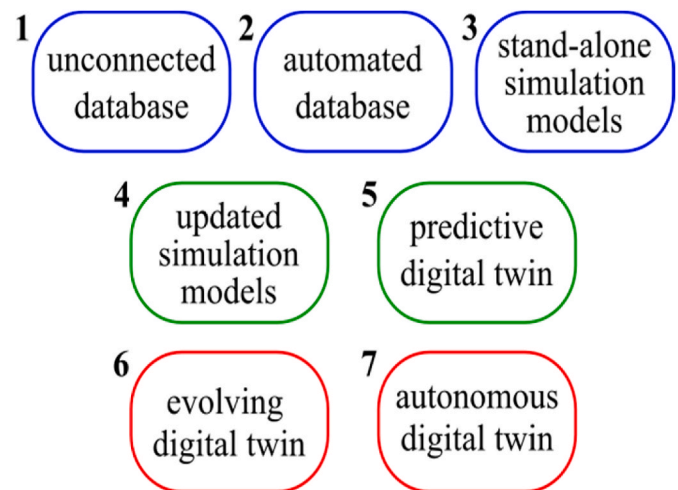

Fig. 7. Evolution of "digital twins" from stand-alone databases and models (1–3), through models updated from measurement data (4–5), to automatically updated digital twins (6–7).

Note that the required input data increases drastically in each step: alarm limits require one parameter, meta-models require wheel and rail profiles, and full simulations complete representations of track and vehicles. A risk here is that the "calibration" of the complex predictive model detaches it from the physical characteristics of the components. This is not necessarily a bad thing – taking the approach a step further would lead to artificial intelligence (AI) approaches where measured input data are related to observed deterioration without any consideration of physical causation. However, both AI analyses and detailed simulations calibrated towards network deterioration provide an "average" response. They are therefore not well suited to identify extreme responses or safety risks etc. Also, AI analyses identify correlation based on historical data. This does not necessarily imply causality, and the models may not be able to capture consequences of altered operational conditions. For these reasons, a combination of physical modelling and data analysis is preferred. Physical modelling is then preferably performed as smaller analyses to investigate key phenomena in detail, whereas the data analysis preferably is carried out on a larger scale to identify overall trends.

8. Railway asset management and risk analysis

Asset management is a core activity for all infrastructure managers and train owners. How the asset management has been organised has however varied significantly. The intention of the ISO 55000 series [1] of standards is to streamline asset management by ensuring a systematic and documented system that can be audited. ISO 55000 is very broad, but provides limited guidance regarding implementation [3]. The present overview focuses on some key aspects related to wheel and rail health management. A more overall guideline for railway related asset management including also organisational and administrative issues is provided in Ref. [68].

8.1. ISO 55000 in relation to mechanical deterioration of railways

ISO 55000 sets out from an asset management policy, and a strategic asset management plan (SAMP) that describes its implementation. The SAMP is broken down to specific asset management plans that specify methods and criteria to take decisions. They also prioritise activities and resources, and specify how results will be evaluated.

When changes in asset management occur – in the current context due to the introduction of new vehicles, change of maintenance contractor etc. – ISO 55000 stresses the importance of risk assessment and control. Incidents, emergencies and unexpected events are indications of flaws in the asset management system. For such events, investigations should be made to identify improvements, to prevent recurrence, and to mitigate effects, see section 8.2.

The standard has strict demands on information management. This includes information necessary for the asset management system to be efficient. Examples are current status and predicted future deterioration of the assets, which relate to demands in ISO 55001 [2] on performance evaluation. Here, the first requirement is to determine what needs to be monitored and measured. For these parameters, "methods for monitoring, measurement, analysis and evaluation, as applicable, to ensure valid results" should be determined. This includes timing of measurements and evaluations. Note the important connection to the discussion in section 7: Neither a too detailed (deterioration) analysis with too high uncertainty in input data, nor a too simplified analysis will "ensure valid results".

There is also a requirement to evaluate and report asset performance, and the effectiveness of the asset management system, including its risk management. The latter also relates to requirements to "establish processes to proactively identify potential failures in asset performance", and evaluate which proactive actions that are suitable. The approach proposed in Ref. [3] essentially sets out from an inventory of asset classes. Potential risks and pertinent (existing and planned) risk controls

are identified. Risks are then analysed. Probability and consequences are evaluated to establish a risk level and whether (and how) this level evolves over time – for assets subjected to mechanical deterioration it will usually get worse. Risks with a low probability but very severe consequences are often overlooked. It is therefore emphasised that the asset management system shall monitor and evaluate the probabilities also for such events.

Finally [3] stresses that outsourcing should in essence not change the demands on the asset management system. This means that the higher the level of outsourcing, the more essential it becomes to control the supplier. Outsourcing also requires the outsourcing organisation to consider involved risks – especially such that cannot be transferred, such as deteriorated public relations due to operational disturbances.

8.2. Risk analyses

Accurate risk analyses are essential in maintaining railway safety. As discussed above, they are also a requirement in ISO 55000. Risk analyses commonly set out from the structure of the common safety method for risk analyses (CSM-RA), which is required in the EU, see Refs. [69–71]. To facilitate implementation in the railway sector, the European Railway Agency has compiled a guideline [72] that contains a detailed comment of [71].

In short, risk analyses should be performed when there are significant changes (as defined in Ref. [71]) that may affect the safety of the (railway) system. The process comprises three main parts:

- System definition
  Factors that define the system to be assessed are described.
- Risk analysis with three possible paths:
  a. Use existing codes of practice
     Usually the most efficient approach if applicable codes exist. Note that codes commonly are often only applicable for new constructions. They may also be inappropriate for very innovative solutions.
  b. Use of a reference system
     This approach raises two questions: How similar are the systems, and how safe is the reference system? Regarding similarity, the main challenge is to identify if and how differences (e.g., in track support conditions) affect the risks. Regarding the level of safety it should be noted that when demands on safety are very high, basing the risk evaluation on statistics becomes very hard (if not impossible): For a risk level of 10^{-6}, on a reference structure where 100 trains pass every day it would on average take 27 years before an accident occurs. It would of course be unrealistic to wait until such a safety level has been statistical ensured. Consequently, the risk evaluation has to consider investigations carried out in designing the reference system. These can then be complemented with additional analyses, measurements, and assessments of any incidents.
  c. Explicit risk estimation
     The most complex approach where simulations and analyses to estimate the risk usually need to be complemented by validating measurements. Some challenges are to identify all relevant failure modes, and to obtain sufficiently reliable input data for the analyses. For progressing mechanical deterioration (as related to the phenomena discussed here, but not e.g., to track buckling), safety can relate to limiting the increase in deterioration between inspections ('defect tolerant') in contrast to ensuring sufficient safety during the entire operational life ('safe life').
- Risk evaluation
  Here it is assessed whether the risk is acceptable. In general this corresponds to ensuring better or similar as the current safety level, or that a certain absolute risk level is attained. The first case is complicated by the fact that current levels often are unknown and likely to vary significantly between different parts of the railway

system. The latter approach is complicated by the difficult assessment (see above) and that the allowed risk level should be related to potential consequences of accidents. These may be hard to foresee and even harder to quantify.

9. Concluding remarks

In short, the paper investigates mechanical deterioration of rails and wheels with the objective to quantify, predict and manage overall health evolution. Suitable parameters, and their relation to predictive analyses and monitoring strategies, are outlined for important deterioration phenomena.

The paper shows how monitoring and predictive analyses relate to the design of digital twins (on different levels), and how the strategy fits into an asset management system. Here it is emphasised that a combination of physical modelling and data analysis should be employed. The benefit of smaller, but better controlled simulations to establish maintenance and safety limits is highlighted. The paper finally relates the approaches to assess and predict wheel/rail deterioration to key demands in the ISO 55000 standard on asset management. Here also demands in standards for risk analyses, and some challenges related to these are discussed.

Declaration of competing interest

The authors declare the following financial interests/personal relationships which may be considered as potential competing interests: Anders Ekberg reports financial support was provided by Shift2Rail and CHARMEC. Elena Kabo reports financial support was provided by Shift2Rail and CHARMEC. Roger Lunden reports financial support was provided by Shift2Rail and CHARMEC. Anders Ekberg and Roger Lundén have been guest editors to Wear. Anders Ekberg is chairperson of the International Scientific Committee of the CM Conference Series.

Data availability

No data was used for the research described in the article.

References

[1] ISO, Asset Management — Overview, Principles and Terminology, International Organization for Standardization, 2014.
[2] ISO, Asset Management – Management Systems – Requirements, International Organization for Standardization, 2014.
[3] ISO, Asset Management – Management Systems – Guidelines for the Application of ISO 55001, International Organization for Standardization, 2014.
[4] A. Ekberg, B. Åkesson, E. Kabo, Wheel/rail rolling contact fatigue – probe, predict, prevent, Wear 314 (2014) 2–12.
[5] N.E. Dowling, S.L. Kampe, M.V. Kral, Mechanical Behavior of Materials, Pearson Education Limited, 2019.
[6] B. Paulsson, A. Ekberg, L. Elfgren, Upgrading of freight railways to meet operational and market demands, in: 7th Transport Research Arena, TRA 2018, 2018. Vienna, Austria, April 16–19, 2018.
[7] B. Paulsson, M. Thunborg, B.-L. Nelldahl, T. Ferriera, S. Escriba Marin, M. Roderiges Placa, J. Nielsen, L. Elfgren, E. Kabo, A. Ekberg, others, D11.5 - Upgrading of Infrastructure in Order to Meet New Operation and Market Demands, Capacity4Rail, 2017.
[8] K. Karttunen, E. Kabo, A. Ekberg, Numerical assessment of the influence of worn wheel tread geometry on rail and wheel deterioration, Wear 317 (2014) 77–91.
[9] K. Karttunen, E. Kabo, A. Ekberg, Estimation of gauge corner and flange root degradation from rail, wheel and track geometries, Wear 366 (2016) 294–302.
[10] S.L. Grassie, J. Kalousek, Rail corrugation: characteristics, causes and treatments, Proc IMechE Part F: J. Rail and Rapid Transit. 207 (1993) 57–68.
[11] S.L. Grassie, Rail corrugation: characteristics, causes, and treatments, Proc IMechE Part F: J. Rail and Rapid Transit. 223 (2009) 581–596.
[12] A. Johansson, Out-of-round Railway Wheels - Causes and Consequences an Investigation Including Field Tests, Out-Of-Roundness Measurements and Numerical Simulations, PhD Thesis, Chalmers University of Technology, 2005.
[13] S.L. Grassie, Rail corrugation: advances in measurement, understanding and treatment, Wear 258 (2005) 1224–1234.
[14] E.G. Berggren, M.X. Li, J. Spännar, A new approach to the analysis and presentation of vertical track geometry quality and rail roughness, Wear 265 (2008) 1488–1496.
[15] M. Maglio, M. Asplund, J.C. Nielsen, T. Vernersson, E. Kabo, A. Ekberg, Digitalisation of condition monitoring data as input for fatigue evaluation of wheelsets, in: Proceedings of the XIX International Wheelset Congress (IWC2019), 2019, pp. 16–20.
[16] G.S. Schajer, Practical Residual Stress Measurement Methods, John Wiley & Sons, 2013.
[17] J. Ahlström, E. Kabo, A. Ekberg, Temperature-dependent evolution of the cyclic yield stress of railway wheel steels, Wear 366–367 (2016) 378–382.
[18] K.L. Johnson, The strength of surfaces in rolling contact, Proc IMechE Part C, J. Mech. Eng. Sci. 203 (1989) 151–163, https://doi.org/10.1243/PIME.
[19] K.A. Meyer, Evaluation of material models describing the evolution of plastic anisotropy in pearlitic steel, Int. J. Solid Struct. 200 (2020) 266–285.
[20] D. Gren, Effect of Large Shear Deformation on Fatigue Crack Behavior in Pearlitic Rail Steel, PhD Thesis, Chalmers University of Technology, Sweden, 2022.
[21] J.F. Archard, Contact and rubbing of flat surfaces, J. Appl. Phys. 24 (1953) 981–988.
[22] M.C. Burstow, Whole Life Rail Model Application and Development for RSSB – Continued Development of an RCF Damage Parameter, Rail Safety & Standards Board, 2004.
[23] B. Dirks, R. Enblom, Prediction model for wheel profile wear and rolling contact fatigue, Wear 271 (2011) 210–217, https://doi.org/10.1016/j.wear.2010.10.028.
[24] R. Lewis, U. Olofsson, Mapping rail wear regimes and transitions, Wear 257 (2004) 721–729.
[25] M. Hiensch, M. Steenbergen, Rolling contact fatigue on premium rail grades: damage function development from field data, Wear 394 (2018) 187–194.
[26] E.E. Magel, Rolling Contact Fatigue: A Comprehensive Review, US Department of Transportation, Federal Railroad Administration, 2011.
[27] R. Andersson, Squat Defects and Rolling Contact Fatigue Clusters - Numerical Investigations of Rail and Wheel Deterioration Mechanisms, PhD Thesis, Chalmers University of Technology, 2018.
[28] R. Deuce, A. Ekberg, E. Kabo, Mechanical deterioration of wheels and rails under winter conditions – mechanisms and consequences, Proc IMechE, Part F: J. Rail and Rapid Transit. 233 (2019) 640–648.
[29] A. Ekberg, E. Kabo, J.C.O. Nielsen, Allowable wheel loads, crack sizes and inspection intervals to prevent rail breaks, in: Proceedings of the 11th International Heavy Haul Association Conference (IHHA 2015), International Heavy Haul Association, Perth, Australia, 2015, pp. 30–38.
[30] S. Caprioli, T. Vernersson, K. Handa, K. Ikeuchi, Thermal cracking of railway wheels: towards experimental validation, Tribol. Int. 94 (2016) 409–420.
[31] L. Podofillini, E. Zio, J. Vatn, Risk-informed optimisation of railway tracks inspection and maintenance procedures, Reliab. Eng. Syst. Saf. 91 (2006) 20–35.
[32] Innotrack, D4.4.1, Rail Inspection Technologies, 2008. Innotrack.
[33] J.J. Marais, K.C. Mistry, Rail integrity management by means of ultrasonic testing, Fatig. Fract. Eng. Mater. Struct. 26 (2003) 931–938.
[34] S.B. Palmer, S. Dixon, R.S. Edwards, X. Jian, Transverse and longitudinal crack detection in the head of rail tracks using Rayleigh wave-like wideband guided ultrasonic waves, in: Nondestructive Evaluation and Health Monitoring of Aerospace Materials, Composites, and Civil Infrastructure IV, International Society for Optics, Photonics, 2005, pp. 70–80.
[35] D.F. Cannon, K.-O. Edel, S.L. Grassie, K. Sawley, Rail defects: an overview, Fatig. Fract. Eng. Mater. Struct. 26 (2003) 865–886.
[36] R. Edwards, S. Dixon, X. Jian, Characterisation of defects in the railhead using ultrasonic surface waves, NDT E Int. 39 (2006) 468–475.
[37] F.L. di Scalea, I. Bartoli, P. Rizzo, M. Fateh, High-speed defect detection in rails by noncontact guided ultrasonic testing, Transport. Res. Rec. (2005) 66–77, 1916.
[38] M. Pathak, S. Alahakoon, M. Spiryagin, C. Cole, Rail foot flaw detection based on a laser induced ultrasonic guided wave method, Measurement 148 (2019), 106922.
[39] J.E. Garnham, J.H. Beynon, The Early Detection of Rolling-Sliding Contact Fatigue Cracks, Mechanics and Fatigue in Wheel/Rail Contact, 1991, pp. 103–116.
[40] Z. Liu, A.D. Koffman, B.C. Waltrip, Y. Wang, Eddy current rail inspection using AC bridge techniques, J. Res. National Instit. Standards Technol. 118 (2013) 140.
[41] R. Pohl, A. Erhard, H.-J. Montag, H.-M. Thomas, H. Wüstenberg, NDT techniques for railroad wheel and gauge corner inspection, NDT E Int. 37 (2004) 89–94.
[42] J. Rajamäki, M. Vippola, A. Nurmikolu, T. Viitala, Limitations of eddy current inspection in railway rail evaluation, Proc IMechE Part F: J. Rail and Rapid Transit. 232 (2018) 121–129.
[43] M.B. Kishore, J.W. Park, S.J. Song, H.J. Kim, S.G. Kwon, Characterization of defects on rail surface using eddy current technique, J. Mech. Sci. Technol. 33 (2019) 4209–4215.
[44] Y. Gao, G.Y. Tian, K. Li, J. Ji, P. Wang, H. Wang, Multiple cracks detection and visualization using magnetic flux leakage and eddy current pulsed thermography, Sens. Actuat. A: Phys. 234 (2015) 269–281.
[45] R.J. Greene, J.R. Yates, E.A. Patterson, Crack detection in rail using infrared methods, Opt. Eng. 46 (2007), 051013.

[46] I.Z. Abidin, G.Y. Tian, J. Wilson, S. Yang, D. Almond, Quantitative evaluation of angular defects by pulsed eddy current thermography, NDT E Int. 43 (2010) 537–546.

[47] J. Wilson, G. Tian, I. Mukriz, D. Almond, PEC thermography for imaging multiple cracks from rolling contact fatigue, NDT E Int. 44 (2011) 505–512.

[48] U. Netzelmann, G. Walle, A. Ehlen, S. Lugin, M. Finckbohner, S. Bessert, NDT of railway components using induction thermography, in: AIP Conference Proceedings, AIP Publishing LLC, 2016, 150001.

[49] Z. Liu, W. Li, F. Xue, J. Xiafang, B. Bu, Z. Yi, Electromagnetic tomography rail defect inspection, IEEE Trans. Magn. 51 (2015) 1–7.

[50] A. Ekberg, B. Paulsson, INNOTRACK: Concluding Technical Report, International Union of Railways (UIC), 2010.

[51] E. Deutschl, C. Gasser, A. Niel, J. Werschonig, Defect detection on rail surfaces by a vision based system, in: IEEE Intelligent Vehicles Symposium, IEEE, 2004, pp. 507–511, 2004.

[52] K.A. Meyer, D. Gren, J. Ahlström, A. Ekberg, A method for in-field railhead crack detection using digital image correlation, Int. J. Real. Ther. (2022) 1–20.

[53] C. Jessop, J. Ahlström, L. Hammar, S. Fæster, H.K. Danielsen, 3D characterization of rolling contact fatigue crack networks, Wear 366 (2016) 392–400.

[54] A. Ekberg, E. Kabo, H. Andersson, An engineering model for prediction of rolling contact fatigue of railway wheels, Fatig. Fract. Eng. Mater. Struct. 25 (2002) 899–909.

[55] E. Kabo, A. Ekberg, P.T. Torstensson, T. Vernersson, Rolling contact fatigue prediction for rails and comparisons with test rig results, Proc IMechE Part F: J. Rail and Rapid Transit. 224 (2010) 303–317, https://doi.org/10.1243/09544097JRRT343.

[56] A.R.S. Ponter, A.D. Hearle, K.L. Johnson, Application of the kinematical shakedown theorem to rolling and sliding point contacts, J. Mech. Phys. Solid. 33 (1985) 339–362.

[57] Y. Jiang, H. Sehitoglu, A model for rolling contact fatigue, Wear 224 (1999) 38–49.

[58] A. Kapoor, A re-evaluation of the life to rupture of ductile metals by cyclic plastic strain, Fatig. Fract. Eng. Mater. Struct. 17 (1994) 201–219.

[59] M.S. Nezhad, D. Floros, F. Larsson, E. Kabo, A. Ekberg, Numerical predictions of crack growth direction in a railhead under contact, bending and thermal loads, Eng. Fract. Mech. 261 (2022), 108218.

[60] A. Ekberg, Rolling contact fatigue of railway wheels—a parametric study, Wear 211 (1997) 280–288.

[61] S. Beretta, G. Donzella, A. Ghidini, R. Roberti, Contact fatigue propagation of deep defects in railway wheels, in: The 13th European Conference on Fracture Mechanics: Applications and Challenge: 6th-9th September, 2000, Elsevier, 2000.

[62] R. Andersson, J. Ahlström, E. Kabo, F. Larsson, A. Ekberg, Numerical investigation of crack initiation in rails and wheels affected by martensite spots, Int. J. Fatig. 114 (2018) 238–251.

[63] S. Caprioli, T. Vernersson, A. Ekberg, Thermal cracking of a railway wheel tread due to tread braking - critical crack sizes and influence of repeated thermal cycles, Proc IMechE, Part F: J. Rail and Rapid Transit. 227 (2012) 10–18.

[64] J. Sandström, E. Kabo, A. Nissen, J. Fredrik, A. Ekberg, Deterioration of Insulated Rail Joints – a Three-Year Field Study, 2012, pp. 460–467.

[65] J. Sandström, A. Ekberg, Numerical study of the mechanical deterioration of insulated rail joints, Proc IMechE Part F: J. Rail and Rapid Transit. 223 (2009) 265–273.

[66] E. Kabo, A. Ekberg, M. Maglio, Rolling contact fatigue assessment of repair rail welds, Wear 436 (2019), 203030.

[67] A. Skyttebol, Continuous Welded Railway Rails: Residual Stress Analyses, Fatigue Assessments and Experiments, PhD Thesis, Chalmers University of Technology, 2004.

[68] UIC, UIC Railway Application Guide – Practical Application of Asset Management through ISO 55001, International Union of Railways, 2016.

[69] European Commission, Commission Implementing Regulation (EU) No 402/2013 of 30 April 2013 on the Common Safety Method for Risk Evaluation and Assessment and Repealing Regulation (EC) No 352/2009 Text with EEA Relevance, 2013.

[70] European Commission, Commission Implementing Regulation (EU) 2015/1136 of 13 July 2015 Amending Implementing Regulation (EU) No 402/2013 on the Common Safety Method for Risk Evaluation and Assessment (Text with EEA Relevance), 2015.

[71] European Commission, Commision Regulation (EC) No 352/2009 on the Adoption of a Common Safety Method on Risk Evaluation and Assessment as Referred to in Article 6(3)(a) of Directive 2004/49/EC of the European Parliament and of the Council, 2009.

[72] D. Jovicic, Guide for the Application of the Commission Regulation on the Adoption of a Common Safety Method on Risk Evaluation and Assessment as Referred to in Article 6 (3)(a) of the Railway Safety Directive, 2009.